Current-voltage characteristics simulation and analysis of 4H-SiC metal-semiconductor-metal ultraviolet photodetectors

Junqin Zhang (张军琴), Yintang Yang (杨银堂), Lifei Lou (娄利飞), and Yan Zhao (赵 妍)

School of Microelectronics, Xidian University,
Key Lab of Ministry of Education for Wide Bandgap Semiconductor Materials and Devices, Xi'an 710071

Received December 26, 2007

The current-voltage (I-V) characteristics of 4H-SiC metal-semiconductor-metal (MSM) ultraviolet photodetector with different finger widths and spacings, different carrier concentrations and thicknesses of n-type epitaxial layer are simulated. The simulation results indicate that the dark current and the photocurrent both increase when the finger width increases. But the effect of finger width on the dark current is more significant. On the other hand, the effect of finger spacing on the photocurrent is more significant. When the finger spacing increases, the photocurrent decreases and the dark current is almost changeless. In addition, it is found that the smaller the carrier concentration of n-type epitaxial layer is, the smaller the dark current and the larger the photocurrent will be. It is also found that I-V characteristics of MSM detector also depend on the epitaxial layer thickness. The dark current of detector is smaller and the photocurrent is larger when the epitaxial layer thickness is about 3 μm.

OCIS codes: 040.5160, 250.0250, 160.6000.
doi: 10.3788/COL20080608.0615.

As a wide bandgap semiconductor material, SiC has advantages in large bandgap, high critical breakdown electric field, high saturation velocity, high heat conductivity, and strong anti-radiation ability. It is a promising material for high-power, anti-radiation electronics devices. Due to the wide bandgap of SiC, the leakage current can be many orders of magnitude lower than that of Si detectors, making SiC good candidates for high sensitivity visible blind ultraviolet (UV) detection[1]. 4H-SiC has a bandgap of 3.26 eV, detectors based on it are intrinsically immune to visible background light[2] and with no responsivity to infrared radiation, which is important for certain applications whenever it is desirable to detect UV in an infrared and visible background[3]. 4H-SiC detectors also have excellent radiation hardiness and very low noise, which is critical for applications in a harsh radiation environment and applications where signals are extremely weak[4]. SiC UV detectors are very attractive in radar, communication, astronomy, military, and photolithography applications which have attracted much attention in recent years.

In the past few years, various types of photodetectors were proposed, such as photoconductor, metal-semiconductor-metal (MSM) photodiode, Schottky barrier detector, p-n junction photodiode, p-i-n junction photodiode, avalanche photodiode, and heterogeneity junction. Among them, MSM photodetector is an attractive choice for UV detection[5]. It has the strongpoint of high responsibility, quick speed, small change with the applied voltage, simple technology of fabrication, and easy monolithic integration[6]. MSM Schottky contact structure is linear interpolation using planar electrode and the semiconductor epitaxial material, which forms two "back-to-back" Schottky barrier. Given a direct current (DC) bias, one barrier is a positive bias, another is a reverse bias. Interdigitated MSM structure plays an important role in both the detection/generation of ultrashort optical/electrical pulses[7]. The property parameters of MSM photodetector, such as quantum efficiency and response time, are close related to the parameters of electrode geometry and optical absorption layer thickness, etc. There are often some contradictions in these parameters[8]. In an actual design of the device, these parameters should be considered. Some results have been achieved in MSM photodetector design and production, but various laboratories are generally based on experience to set their own[9]. This is obviously different to the aim of the high performance MSM detector.

Current-voltage (I-V) characteristic is an important electrical property of UV photodetector, which directly reflects the sensitivity of the detector. Based on the relevant models of 4H-SiC material and devices, MSM UV detector model for 4H-SiC is proposed in this letter. The room temperature I-V characteristics of 4H-SiC MSM detector with different finger widths and spacings, different carrier concentrations and thicknesses of n-type epitaxial layer are simulated with the two-dimensional (2D) device simulator Medici. The effects of them on I-V characteristics of photodetector are discussed.

Medici is a powerful device simulation program that can be used to simulate the behavior of semiconductor device[10]. The program solves Poisson's equation and both the electron and hole current-continuity equations to obtain the electric potential distribution and carrier distribution before and after the light illumination respectively. The Medici optical device advanced application module (OD-AAM) is used to model propagation of light inside and outside a device.

A 4H-SiC UV detector model is developed. We adopt a drift-diffusion model which consists of the Poisson's equation, continuity equations, and Boltzmann transport theory. In addition, the mobility model is used. The mobility model presently available in Medici can be classified into three categories: low field, transverse field, and parallel field, which are applied to different situations. In our simulation, the low field mobility model is chosen. By exposing a SiC detector structure to light, it is possible to generate electron-hole pairs inside the device. There is a recombination in the course of photo-generated carrier transportation. Shockley-Read-Hall (SRH) and Auger recombinations are considered in the simulation. The level of impurities in SiC is deeper, impurities will not be completely ionized at room temperature or even higher temperatures, so impurities incomplete ionization effect is considered in device simulation. Medici supports four types of basic boundary conditions. In the contact between metal and semiconductor, Schottky contact forms for MSM Schottky detector, so the Schottky contacts is considered. In addition, photogeneration model and absorption model are also used in our simulation.

Figure 1 is the schematic structure of 4H-SiC MSM UV detector in our simulation. The UV detector is fabricated on a 3.5-μm-thick n-type 4H-SiC epitaxial layer, with a doping concentration of 3×10^{15} cm^{-3}, which grows on a 400-μm-thick, 5×10^{18} cm^{-3} doped n$^+$ 4H-SiC substrate. Schottky contacts on the epitaxial layer are formed by defining a 200-nm-thick Ni interdigitated contact electrode. Due to its high optical transmittance in the UV range, indium tin oxide (ITO) transparent layers of appropriate thickness are then deposited between the metal stripes as an anti-reflection coating.

Based on the relevant models of 4H-SiC material and device, a UV detector model is developed, and the *I*-*V* characteristics and spectral response of 4H-SiC MSM UV photodetectors are simulated with the 2D device simulator Medici[11]. It is shown that the simulation results agree with the experimental data very well, which proves the validity of this model. On the basis of the established model, we study the *I*-*V* characteristics of 4H-SiC MSM UV photodetectors with different physical parameters.

Figures 2 and 3 show *I*-*V* characteristics of detectors with different finger widths. Two types of detector topology are shown with 2- and 5-μm spacings between contact fingers. It can be seen that the dark current increases with the increase of finger width. With a DC bias of 10 V, the dark current density is only 8.7×10^{-14} A/μm when the finger width is 0.5 μm, but it is up to 9.7×10^{-13} A/μm when the finger width is 10 μm. Furthermore, the shape of dark *I*-*V* curves is homology and the values of dark current are almost equivalent when the spacings between contact fingers are 2 and 5 μm, respectively. It is found that the photocurrent increases

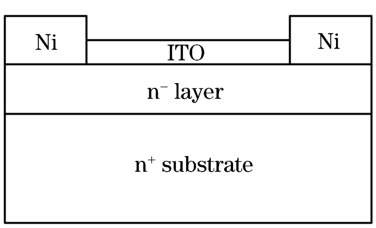

Fig. 1. Schematic structure of SiC UV detector.

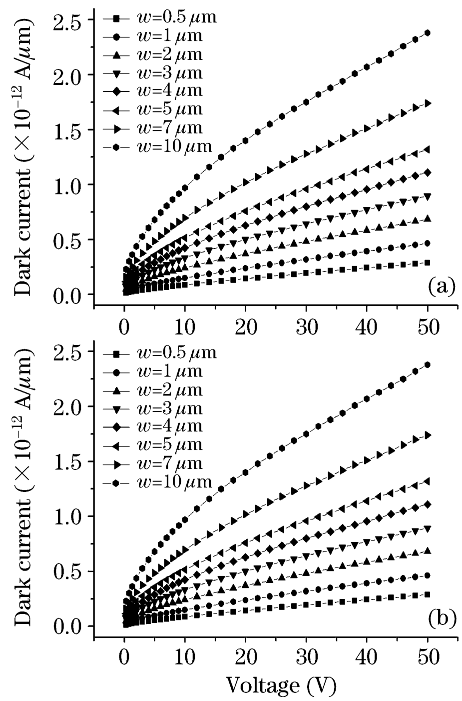

Fig. 2. Dark *I*-*V* characteristics of MSM detector with different finger widths. The spacing between contact fingers is (a) 2 μm and (b) 5 μm. *w*: finger width.

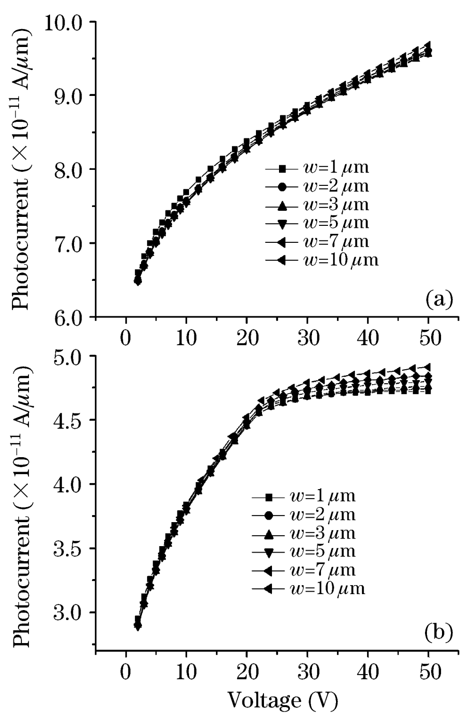

Fig. 3. Photo *I*-*V* characteristics of MSM detector with different finger widths. The spacing between contact fingers is (a) 2 μm and (b) 5 μm. *w*: finger width.

with the increase of finger width at a given bias because the effective illuminated area is larger. It is also found that the photocurrents are 7.7×10^{-11} and 3.7×10^{-11} A/μm at 10-V bias when the spacings between contact fingers are 2 and 5 μm, respectively. In other words, the photocurrent increases when the finger spacing reduces at a given bias because the collection efficiency is improved. These conclusions are consistent with the experimental results of Ref. [12]. The magnitudes of dark current and the photocurrent in the MSM 4H-SiC UV photodetector are also consistent with the experimental results of Ref. [13].

Figure 4 shows the dark *I*-*V* characteristics of the detector with different finger spacings. It can be seen that the dark current is almost invariable with the increase of finger spacing. It is also found that the dark current of detector with 5-μm finger width is larger than that with 2-μm finger width. This also agrees with the conclusion from Fig. 2.

Figure 5 shows the photo *I*-*V* characteristics of the detector with different finger spacings. It is found that the photocurrent increases with the finger spacing reducing, which is consistent with the results from Fig. 3 and the experimental results of Ref. [12].

Figure 6 shows the *I*-*V* characteristics of the MSM 4H-SiC UV detector using the carrier concentration as variable. The epitaxial layer thickness, the finger width and spacing are 2, 2, and 5 μm, respectively. It can be seen that the dark current increases with the increase of carrier concentration except for 5×10^{17} cm^{-3}. But the photocurrent decreases with the increase of carrier concentration. This verifies that the smaller the background carrier concentration the greater the photocurrent.

The effect of epitaxial layer thickness on the *I*-*V* characteristics of MSM 4H-SiC UV detector is also investigated and shown in Figs. 7 and 8. The finger width of detector is 2 μm and the spacing is 5 μm. It can be seen that with the increase of carrier concentration, the influence of epitaxial layer thickness on the dark current and photocurrent decrease. It is also found that the

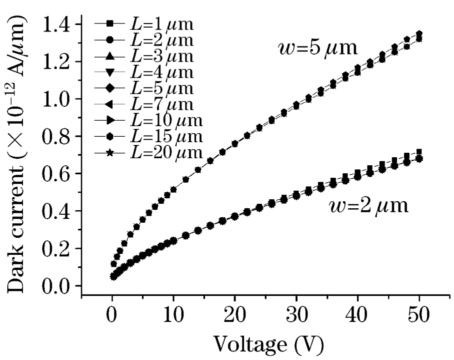

Fig. 4. Dark *I*-*V* characteristics of MSM detector with different finger spacings. *L*: finger spacing.

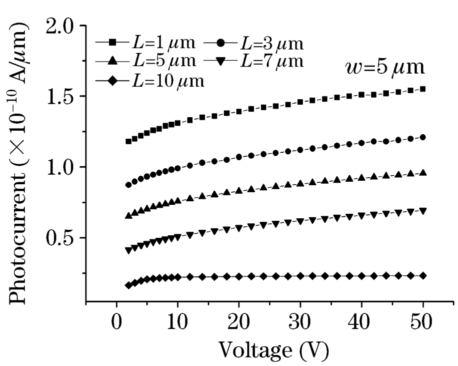

Fig. 5. Photo *I*-*V* characteristics of MSM detector with different finger spacings. *L*: finger spacing.

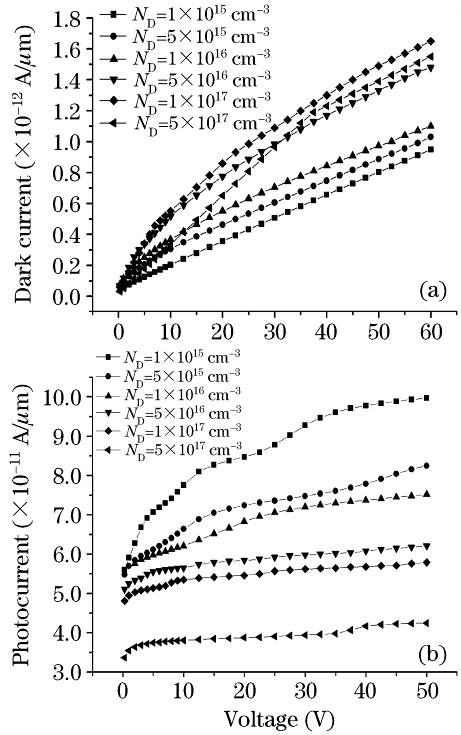

Fig. 6. *I*-*V* characteristics of MSM detector with different carrier concentrations. (a) Dark *I*-*V* characteristics; (b) photo *I*-*V* characteristics. N_{D}: carrier concentration.

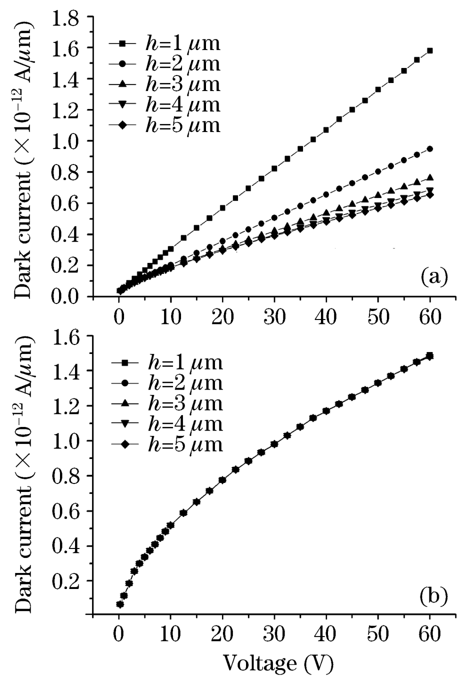

Fig. 7. Dark *I*-*V* characteristics of MSM detector in different epitaxial layer thicknesses. (a) $N_{\mathrm{D}} = 1 \times 10^{15}$ cm^{-3}; (b) $N_{\mathrm{D}} = 5 \times 10^{16}$ cm^{-3}. *h*: epitaxial layer thickness.

photocurrent is minimum when epitaxial layer thickness is 1 μm, and it gradually increases when the epitaxial layer thickness increases. By choosing adequate thickness of the epitaxial layer, the performance of the MSM detector could be improved. Epitaxial layer should not be too thick or too thin because excessive active layer not only needs long growth time of epitaxial layer but also affects

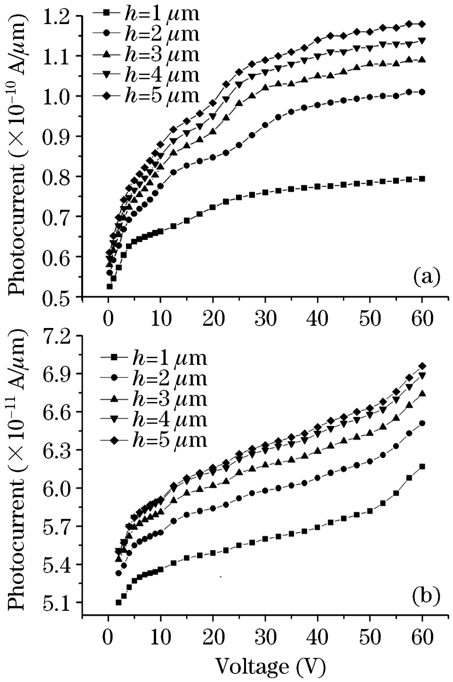

Fig. 8. Photo *I-V* characteristics of MSM detector with different epitaxial layer thicknesses. (a) $N_D = 1 \times 10^{15}$ cm^{-3}; (b) $N_D = 5 \times 10^{16}$ cm^{-3}. *h*: epitaxial layer thickness.

the transient response of detector. And the thickness of the inferior active layer reduces the opto-electric sensitivity because of insufficient photo-absorption. From Figs. 7 and 8, it can be seen that the MSM detector shows the optimum *I-V* characteristics when the epitaxial layer thickness is about 3 μm.

In summary, the *I-V* characteristics of 4H-SiC MSM UV photodetector with different finger widths and spacings, different carrier concentrations and thicknesses of n-type epitaxial layer are simulated. The results are helpful to design wide-bandgap semiconductor-material MSM UV detector. Furthermore, in order to get high-performance UV detector, we should choose suitable parameters.

This work was supported by the National Defense Pre-Research Foundation of China. J. Zhang's e-mail address is zhangjunqin@sina.com.

References

1. F. Yan, X. Xin, S. Aslam, Y. Zhao, D. Franz, J. H. Zhao, and M. Weiner, IEEE J. Quantum Electron. **40,** 1315 (2004).
2. Y. Zhou, Y. Zhang, Y. Zhang, and X. Meng, Acta Phys. Sin. (in Chinese) **53,** 3710 (2004).
3. D. M. Brown, E. T. Downey, M. Ghezzo, J. W. Kretchmer, R. J. Saia, Y. S. Liu, J. A. Edmond, G. Gati, J. M. Pimbley, and W. E. Schneider, IEEE Trans. Electron Devices **40,** 325 (1993).
4. X. Xin, F. Yan, T. W. Koeth, C. Joseph, J. Hu, J. Wu, and J. H. Zhao, Electron. Lett. **41,** 1192 (2005).
5. C. K. Wang, S. J. Chang, Y. K. Su, Y. Z. Chiou, S. C. Chen, C. S. Chang, T. K. Lin, H. L. Liu, and J. J. Tang, IEEE Trans. Electron Devices **53,** 38 (2006).
6. X. Yang, B. Liu, Y. Ma, B. Zhao, Y. Zhang, T. Yang, H. Yang, W. Li, D. Liu, and G. Du, Chin. J. Luminescence (in Chinese) **25,** 156 (2004).
7. T. O. Körner, P. Regli, U. Krumbein, and W. Fichtner, in *Proceedings of 1996 Lasers and Electro-Optics Society Annual Meeting* **1,** TuG3, 186 (1996).
8. X. Chen, "The research and fabrication of GaN-based materials and MSM UV-photodetectors" Master's Degree Thesis (Xiamen University, 2002) p.23.
9. L. Liu, "Study of ohmic contact and MSM UV detector based on GaN" Master's Degree Thesis (Zhejiang University, 2004) p.43.
10. Avant Corporation, TCAD Business Unit, Avant Corporation Medici User's Manual (1998).
11. J. Zhang, Y. Yang, Y. Lu, L. Lou, and Y. Zhao, Chinese J. Lasers (in Chinese) **35,** 509 (2008).
12. M. Mosca, J.-L. Reverchon, N. Grandjean, and J.-Y. Duboz, IEEE J. Sel. Top. Quantum Electron. **10,** 752 (2004).
13. Z. Wu, X. Xin, F. Yan, and J. Zhao, Chin. J. Quantum Electron. (in Chinese) **21,** 269 (2004).